

# Variational wave functions for the Mott-Hubbard transition

Autor(en): **Dzierzawa, M. / Baeriswyl, D. / Martelo, L.M.**

Objektyp: **Article**

Zeitschrift: **Helvetica Physica Acta**

Band (Jahr): **70 (1997)**

Heft 1-2

PDF erstellt am: **11.09.2024**

Persistenter Link: <https://doi.org/10.5169/seals-117015>

## **Nutzungsbedingungen**

Die ETH-Bibliothek ist Anbieterin der digitalisierten Zeitschriften. Sie besitzt keine Urheberrechte an den Inhalten der Zeitschriften. Die Rechte liegen in der Regel bei den Herausgebern. Die auf der Plattform e-periodica veröffentlichten Dokumente stehen für nicht-kommerzielle Zwecke in Lehre und Forschung sowie für die private Nutzung frei zur Verfügung. Einzelne Dateien oder Ausdrucke aus diesem Angebot können zusammen mit diesen Nutzungsbedingungen und den korrekten Herkunftsbezeichnungen weitergegeben werden. Das Veröffentlichen von Bildern in Print- und Online-Publikationen ist nur mit vorheriger Genehmigung der Rechteinhaber erlaubt. Die systematische Speicherung von Teilen des elektronischen Angebots auf anderen Servern bedarf ebenfalls des schriftlichen Einverständnisses der Rechteinhaber.

## **Haftungsausschluss**

Alle Angaben erfolgen ohne Gewähr für Vollständigkeit oder Richtigkeit. Es wird keine Haftung übernommen für Schäden durch die Verwendung von Informationen aus diesem Online-Angebot oder durch das Fehlen von Informationen. Dies gilt auch für Inhalte Dritter, die über dieses Angebot zugänglich sind.

# Variational Wave Functions for the Mott-Hubbard Transition

By M. Dzierzawa <sup>(1)</sup>, D. Baeriswyl <sup>(1)</sup> and L. M. Martelo <sup>(1,2)</sup>

(1) Institut de physique théorique, Université de Fribourg, Pérolles, CH-1700 Fribourg, Switzerland

(2) Department of Physics, University of Évora, Portugal

(9.VII.1996)

*Abstract.* The Hubbard model is investigated at half-filling as a function of the interaction strength  $U$ , using two different variational wave functions. The first, due to Gutzwiller, describes a metallic phase, the second an antiferromagnetic insulator. The comparison of the variational energies yields a transition between a metallic phase for small  $U$  to an insulating phase at large  $U$ . Three different cases are discussed in some detail, the one-dimensional chain with long-range hopping (the  $1/r$  Hubbard model), and both the hypercubic and hyperdiamond lattices in the limit of infinite dimensions.

## 1 Introduction

Materials can be roughly divided into two classes: insulators and metals. However, this classification is not always clear-cut since there exist various mechanisms which can drive a given system into one of the two regimes: band structure effects, Fermi surface instabilities, localization due to disorder, polaronic effects. Moreover, in many cases a system may be insulating or metallic, depending on the values of certain parameters such as pressure, temperature, composition, magnetic field, and others. The variation of one of these parameters may then induce a transition from a metallic to an insulating regime [1].

From a theoretical point of view the most intricate case appears to be the metal-insulator transition induced by electron-electron correlations. This mechanism has first been discussed by Mott in terms of a lattice of hydrogen atoms with variable lattice constant [2], subse-

quently it was studied mostly in terms of the single-band Hubbard model [3, 4]. This "Mott phenomenon" is also believed to play an essential role in the physics of high-temperature superconductors [5].

The Mott-Hubbard metal-insulator transition can be pictured as follows. For small bandwidth (i.e. large separation between atoms) there is a "Coulomb blockade" due to the large energy required for putting two electrons on a single atom. This prevents electrons from moving and renders the system insulating. For large bandwidth the gain in energy due to delocalization of the single-electron states removes the Coulomb blockade, and the system is metallic.

An alternative view has been proposed by Slater who discovered that antiferromagnetic ordering leads to band splitting and therefore also to a metal-insulator transition, which can be described already on a simple one-electron level, using the Unrestricted Hartree-Fock (UHF) approximation [6].

Recently the interplay between the Mott phenomenon and antiferromagnetic order has become more clear, thanks to new computational techniques and the development of a "dynamical mean-field theory", formally derived by taking the limit of infinite dimensions [7]. According to these results it is difficult to suppress the antiferromagnetic ordering at low temperatures, and in most cases the metal-insulator transition can be viewed as a Fermi surface instability with respect to a spin-density wave ground state (an antiferromagnetic state with small local moments). However, at high temperatures and in situations where the antiferromagnetism is suppressed by frustration or by quantum fluctuations the Mott-Hubbard transition can be clearly observed, not only in numerical simulations, but also in real experiments, for instance on the model substance  $V_2O_3$  [7].

In this paper we consider the Hubbard model on a  $d$ -dimensional lattice

$$\hat{H} = \hat{T} + U\hat{D} \quad (1.1)$$

where

$$\hat{T} = - \sum_{i,j} t_{ij} \hat{c}_{i\sigma}^+ \hat{c}_{j\sigma} \quad (1.2)$$

transfers electrons between the sites of the lattice and

$$\hat{D} = \sum_i \hat{n}_{i\uparrow}^+ \hat{n}_{i\downarrow} \quad (1.3)$$

measures the number of doubly occupied sites. The operators  $\hat{c}_{i\sigma}^+$  ( $\hat{c}_{i\sigma}$ ) create (annihilate) electrons on site  $i$  with spin projection  $\sigma$  and  $\hat{n}_{i\sigma} = \hat{c}_{i\sigma}^+ \hat{c}_{i\sigma}$ .

We limit ourselves to the case of a half-filled band (one electron per site on average). Therefore the metal-insulator transition induced by doping a Mott-Hubbard insulator is not considered here, although this problem remains one of the most important issues in condensed matter theory. Furthermore we study only the zero-temperature limit. The only remaining parameters are then the symmetry of the lattice, its dimensionality  $d$  and the relative strength of the interaction  $U/W$ , where  $W$  is the bandwidth.

The Hubbard model at half filling embodies the Mott phenomenon as follows. For  $U \rightarrow \infty$  all sites are singly occupied and no free charge carriers are available: the system is insulating. For large but finite  $U$  holes and doubly occupied sites appear, but they will be bound in pairs. Both the number and the size of these particle-hole pairs steadily increase with decreasing  $U$  and, correspondingly, the dielectric constant increases until, at a critical value  $U_c$ , it diverges. Below this value free "particles" (doubly occupied sites) and holes exist, and the system is metallic.  $U_c$  is expected to be of the order of the bandwidth  $W$ .

In order to describe this transition quantitatively, we use two complementary types of variational wave functions, one linked to the exact ground state for  $U = 0$  (Gutzwiller wave function), the other connected to the exact ground state of the  $U \rightarrow \infty$  limit. These wave functions are introduced in Section 2 and shown to be, respectively, metallic and insulating. In Section 3 our variational scheme is applied to infinite-dimensional lattices (both hypercubic and hyperdiamond), where the calculations are drastically simplified. In this limit the tendency towards antiferromagnetism is particularly pronounced, since spin fluctuations are strongly suppressed. In Section 4 a one-dimensional chain with long-range hopping (the  $1/r$  model) is investigated. In this case the variational calculation can again be explicitly carried out, but now the metal-insulator transition is of a pure Mott-Hubbard type, since both quantum fluctuations and frustration prevent the system from exhibiting long-range antiferromagnetic order.

## 2 Variational wave functions

Despite its formal simplicity the Hubbard model represents a highly non-trivial many-body problem, where perturbative results have a limited range of validity and exact diagonalizations are restricted to small size systems, at least in two or higher dimensions. The variational principle offers an alternative way for studying ground state properties, as a well-chosen wave function may display essential features without requiring too heavy computations. A very popular ansatz is the wave function introduced by Gutzwiller [8, 9]

$$|\Psi_G\rangle = e^{-\eta\hat{D}}|\Psi_0\rangle \quad (2.1)$$

where  $\eta$  is a variational parameter and  $|\Psi_0\rangle = \prod_{k < k_F, \sigma} \hat{c}_{\mathbf{k}, \sigma}^+ |0\rangle$  is the ground state for  $U = 0$ , i.e. the Fermi sea filled up to the Fermi momentum  $k_F$ . It is instructive to express the Gutzwiller wave function in real space occupation number representation

$$|\Psi_G\rangle = \sum_{\{n_{i\sigma}\}} e^{-\eta \sum_i n_{i\uparrow} n_{i\downarrow}} f(\{n_{i\sigma}\}) |\{n_{i\sigma}\}\rangle \quad (2.2)$$

where the Fermi surface does not show up explicitly but is hidden in the phase correlations of the complex amplitudes  $f(\{n_{i\sigma}\})$ . The Gutzwiller correlator  $e^{-\eta\hat{D}}$  does not destroy these subtle phase correlations, it merely reweighs all configurations with  $D$  doubly occupied sites by an overall factor  $e^{-\eta D}$ , i.e. configurations with large  $D$  are exponentially suppressed. Therefore one expects that for any finite value of  $\eta$  the Gutzwiller wave function will preserve the jump in the momentum distribution function. Only in the limit  $\eta \rightarrow \infty$  one is left with

a fully projected wave function where no doubly occupied sites are left over. In this limit the momentum distribution function is constant,  $\langle \hat{n}_{\mathbf{k}\sigma} \rangle = 1/2$ .

In the large  $U$  limit empty and doubly occupied sites are not distributed homogeneously over the system but rather tend to form pairs, a feature that is completely absent in the Gutzwiller wave function, as noticed some time ago [10]. There have been attempts to cure this defect by introducing further operators in the Gutzwiller wave function, which enhance the nearest correlations between empty and doubly occupied sites. In this way it has been possible to produce much better variational energies in the strong coupling limit, as compared to the original Gutzwiller wave function, but unfortunately expectation values can only be evaluated numerically [11] or using certain approximations [12]. Moreover these wave functions do not represent an insulating ground state, and therefore it is problematic to use them for the strong coupling limit.

In view of the serious shortcomings of the Gutzwiller ansatz in the large  $U$  limit, an alternative variational ground state has been proposed [13] that can be regarded as the strong coupling counterpart of the Gutzwiller wave function. It is defined as

$$|\Psi_B\rangle = e^{-\eta\hat{T}}|\Psi_\infty\rangle$$

where  $|\Psi_\infty\rangle$  is the ground state of the Hubbard model for  $U \rightarrow \infty$ , or, what is equivalent, the ground state of the antiferromagnetic Heisenberg model. It is instructive to rewrite  $|\Psi_B\rangle$  in  $k$ -space occupation number representation, in perfect correspondence to the real space representation for  $|\Psi_G\rangle$ ,

$$|\Psi_B\rangle = \sum_{\{n_{k\sigma}\}} e^{-\eta \sum_{k,\sigma} \epsilon_k n_{k\sigma}} g(\{n_{k\sigma}\}) |\{n_{k\sigma}\}\rangle \quad (2.3)$$

Here  $g(\{n_{k\sigma}\})$  are the coefficients of the antiferromagnetic ground state  $|\Psi_\infty\rangle$  in momentum space representation. The operator  $e^{-\eta\hat{T}}$  suppresses configurations with high kinetic energy  $T = \sum_{k,\sigma} \epsilon_k n_{k\sigma}$ . For small values of  $\eta$  the spin correlations of the variational wave function  $|\Psi_B\rangle$  will resemble very much those of the Heisenberg antiferromagnet since the phase relations among the  $g(\{n_{k\sigma}\})$  are not affected by the operator  $e^{-\eta\hat{T}}$ . In the limit  $\eta \rightarrow \infty$  only the configuration with the lowest kinetic energy, i.e. the Fermi sea, survives. Thus  $|\Psi_B\rangle$  is the exact ground state not only for  $U \rightarrow \infty$  but also in the limit  $U \rightarrow 0$ .

Another way to visualize the nature of  $|\Psi_B\rangle$ , at least for small  $\eta$ , is to expand it in powers of  $\eta$ ,

$$|\Psi_B\rangle = |\Psi_\infty\rangle - \eta\hat{T}|\Psi_\infty\rangle + \frac{\eta^2}{2}\hat{T}^2|\Psi_\infty\rangle - \dots \quad (2.4)$$

The action of  $\hat{T}$  on  $|\Psi_\infty\rangle$ , where there is exactly one electron per site, creates configurations with empty and doubly occupied sites. In the special case of nearest-neighbour hopping,  $\hat{T}$  moves an electron from one site to a neighbouring one. Thus "particle-hole pairs" appear on nearest neighbour sites within the contribution  $\sim \eta$ , while higher order contributions  $\sim \eta^n$  contain pairs separated by at most  $n$  steps. The presence of few and tightly bound pairs for small  $\eta$  characterizes well the ground state for large values of  $U$ . Therefore the

trial state  $|\Psi_B\rangle$  appears to be more natural in this limit than the Gutzwiller wave function supplemented by a correlation factor for particles and holes.

Unfortunately, the state  $|\Psi_\infty\rangle$  is generally not known (in contrast to  $|\Psi_0\rangle$ ), which renders practical calculations for  $|\Psi_B\rangle$  rather difficult. Exact results using  $|\Psi_B\rangle$  are available only for special particular cases: the limit of infinite dimensions and the one-dimensional  $1/r$  Hubbard model. They will be discussed in Sections 4 and 5, respectively.

### 3 Drude weight

How can we decide whether a given wave function is metallic or insulating? A criterion due to Kohn [14], based on the sensitivity of the ground state energy with respect to changes of boundary conditions, is particularly useful in this context since it does not require any information about excited states. For the sake of simplicity we limit ourselves to a one-dimensional system with nearest neighbour hopping (the generalization to arbitrary dimensions is straightforward). Following Kohn, we consider a closed ring of length  $L$  threaded by a flux  $\Phi$ . We associate the flux with a vector potential  $A = \Phi/L$  along the chain. Consequently the hopping matrix elements have to be multiplied by a phase factor and the flux dependent kinetic energy reads

$$\hat{T}(\Phi) = -t \sum_{i,\sigma} \left( e^{i\Phi/L} \hat{c}_{i\sigma}^+ \hat{c}_{i+1,\sigma} + e^{-i\Phi/L} \hat{c}_{i+1,\sigma}^+ \hat{c}_{i,\sigma} \right) \quad (3.1)$$

One can then define a charge stiffness

$$D_c = L \left. \frac{d^2 E(\Phi)}{d\Phi^2} \right|_{\Phi=0}. \quad (3.2)$$

where  $E(\Phi)$  is the ground state energy for a given flux  $\Phi$ . It can be shown [14] that the charge stiffness is proportional to the prefactor in the  $\delta$ -function contribution of the zero temperature conductivity  $\sigma(\omega)$ , the Drude weight. The charge stiffness is finite for a metal and vanishes for an insulator. In the following we show that the Gutzwiller wave function  $|\Psi_G\rangle$  is metallic while the wave function  $|\Psi_B\rangle$  always represents an insulator. We first consider the Gutzwiller wave function. The variational ground state energy for a given flux  $\Phi$  is obtained by minimizing

$$F(\Phi, \eta) = \frac{\langle \Psi_0(\Phi) | e^{-\eta \hat{D}} \hat{H}(\Phi) e^{-\eta \hat{D}} | \Psi_0(\Phi) \rangle}{\langle \Psi_0(\Phi) | e^{-2\eta \hat{D}} | \Psi_0(\Phi) \rangle} \quad (3.3)$$

with respect to  $\eta$ . The result is  $E_G(\Phi) = F(\Phi, \eta(\Phi))$  where  $\eta(\Phi)$  denotes the optimal value of  $\eta$  for a given flux  $\Phi$ . The second derivative of the variational energy with respect to  $\Phi$  yields

$$\frac{d^2 E_G(\Phi)}{d\Phi^2} = \frac{\partial^2 F}{\partial \Phi^2} + 2 \frac{\partial^2 F}{\partial \Phi \partial \eta} \frac{d\eta}{d\Phi} + \frac{\partial^2 F}{\partial \eta^2} \left( \frac{d\eta}{d\Phi} \right)^2 \quad (3.4)$$

where we have already used the minimum condition  $\partial F/\partial\eta = 0$ . In the limit  $\Phi \rightarrow 0$  Eq. (3.4) simplifies further since  $\eta(\Phi)$  is an even function, and therefore  $\partial\eta/\partial\Phi = 0$  at  $\Phi = 0$ . The charge stiffness of the Gutzwiller wave function is thus simply given by the first term of Eq. (3.4),

$$D_c = L \left. \frac{\partial^2 F(\Phi, \eta)}{\partial\Phi^2} \right|_{\Phi=0} \quad (3.5)$$

In order to proceed, it is crucial to realize that the ground state  $|\Psi_0(\Phi)\rangle$  of the non-interacting system does not depend on  $\Phi$  as long as  $\Phi$  is small enough. When a flux  $\Phi$  is applied, the one-particle energy levels  $\epsilon_k$  are shifted to  $\epsilon_{k+\Phi/L}$ , but levels will cross only if  $\Phi \approx 1$ . Therefore the second derivative with respect to  $\Phi$  in Eq. (3.5) acts only on  $\hat{H}(\Phi)$ . Using the fact that  $\partial^2 \hat{H}(\Phi)/\partial\Phi^2 = -\hat{T}(\Phi)/L^2$  we obtain the final result

$$D_c = -\frac{1}{L} \langle \hat{T} \rangle \quad (3.6)$$

The Drude weight for the Gutzwiller wave function is simply proportional to the expectation value of the kinetic energy and therefore vanishes only in the limit of the completely projected state  $\eta \rightarrow \infty$ . This result has previously been obtained by Millis and Coppersmith [15] using slightly different arguments. The conclusion is that the Gutzwiller wave function *alone* cannot be used to investigate the Mott-Hubbard transition.

We now turn to the wave function  $|\Psi_B\rangle$  which is appropriate for the strong coupling limit of the Hubbard model. As before we have to calculate the flux-dependent variational ground state energy  $E_B(\Phi)$  which is obtained by minimizing

$$F(\Phi, \eta) = \frac{\langle \Psi_\infty | e^{-\eta\hat{T}(\Phi)} \hat{H}(\Phi) e^{-\eta\hat{T}(\Phi)} | \Psi_\infty \rangle}{\langle \Psi_\infty | e^{-2\eta\hat{T}(\Phi)} | \Psi_\infty \rangle} \quad (3.7)$$

with respect to  $\eta$ . We will argue that  $E_B(\Phi)$  does not depend on  $\Phi$  at all, and therefore the Drude weight vanishes identically. First of all, we notice that  $|\Psi_\infty\rangle$  does not depend on  $\Phi$ . In the limit  $U \rightarrow \infty$  the Hubbard Hamiltonian can be mapped onto the antiferromagnetic Heisenberg model with exchange coupling  $J \sim |t|^2/U$ , and the phase factor associated with  $\Phi$  cancels out.

Expanding all exponentials appearing in Eq. (3.7) in powers of  $\hat{T}(\Phi)$  one is left with expectation values of the type

$$\langle \Psi_\infty | \hat{T}^n(\Phi) \hat{D} \hat{T}^m(\Phi) | \Psi_\infty \rangle \quad (3.8)$$

The wave function  $|\Psi_\infty\rangle$  is a superposition of states where each site is singly occupied. Acting with  $\hat{T}(\Phi)$  on  $|\Psi_\infty\rangle$  moves an electron from one site to a neighbouring one, thus creating empty and doubly occupied sites in the system. Each move to the right (left) is associated with a phase factor  $e^{i\Phi/L}$  ( $e^{-i\Phi/L}$ ). In order to have a non-vanishing matrix element (3.8) the total number of moves to the left and to the right must be the same, since in the end one has to reach again a state where each site is singly occupied. Therefore all phase factors cancel completely and the matrix elements are independent of  $\Phi$ . Consequently  $E_B(\Phi)$  is

independent of  $\Phi$  and the Drude weight is zero. Thus the wave function  $|\Psi_B\rangle$  describes an insulator.

It seems therefore natural to approach the problem of the Mott-Hubbard transition using *both* wave functions. For small  $U$  the Gutzwiller wave function is expected to have lower energy, whereas for large  $U$  the wave function  $|\Psi_B\rangle$  will be more stable. The value  $U_c$  where both wave functions yield the same variational energy will then locate the metal-insulator transition.

## 4 Infinite dimensions

In view of the difficult tasks encountered in dealing with strongly correlated electrons, it came as a relief when it was recognized that there exists a non-trivial limit of infinite dimensions where the problem is greatly simplified [16]. Presently many properties are already known for the Hubbard model in infinite dimensions, and the physical meaning of this limit as a dynamical mean-field theory for the finite-dimensional case is essentially clear [7].

The variational wave functions presented in Section 2 suffer from similar problems: only in very rare (one-dimensional) cases they can be treated exactly [17, 18]. While for  $|\Psi_G\rangle$  there exist at least reasonable approximations and straightforward numerical techniques (variational Monte Carlo [19]), the situation is even worse for  $|\Psi_B\rangle$  where the fact that  $|\Psi_\infty\rangle$  is not known for  $d > 1$  makes it difficult to proceed beyond an expansion to lowest order in  $t/U$  [13].

Fortunately, in the limit of infinite dimensions both variational wave functions can again be treated exactly. As to the Gutzwiller wave function, Metzner and Vollhardt [16] were able to show that the "Gutzwiller approximation" becomes exact in the limit  $d \rightarrow \infty$ . In this approximation the ground state energy per site is given by

$$\varepsilon_G = \frac{E_G}{L} = \begin{cases} -|\epsilon_0| \left(1 - \frac{U}{U_0}\right)^2 & \text{for } U \leq U_0 \\ 0 & \text{for } U > U_0 \end{cases} \quad (4.1)$$

where  $\epsilon_0$  is the kinetic energy of the Fermi sea (per site) and  $U_0 = 8|\epsilon_0|$ . At  $U_0$  both the number of doubly occupied sites and the discontinuity of the momentum distribution function drop to zero. Therefore, as pointed out by Brinkman and Rice [4], the Gutzwiller approximation predicts a metal-insulator transition at  $U = U_0$ .

In our approach, as will be shown below, this Brinkman-Rice transition does not occur. The (insulating) state  $|\Psi_B\rangle$  is energetically favoured with respect to  $|\Psi_G\rangle$  already below  $U_0$ , and in the entire region  $U < \infty$  the double occupancy remains finite. The variational wave function for the strong coupling limit,  $|\Psi_B\rangle$ , is based on the exact ground state for  $U \rightarrow \infty$ . In the limit of infinite dimensions and for bipartite lattices this is simply the Néel state [20]. We consider two types of bipartite lattices, the hypercubic and the hyperdiamond lattices. The latter is the generalization of the  $2d$  honeycomb and  $3d$  diamond lattices to arbitrary



dimensions. The hopping integrals in Eq. (1.2) are restricted to nearest neighbour sites (tight-binding approximation).

We first consider the hypercubic lattice. In  $k$  representation the Néel state can be written as

$$|\Psi_\infty\rangle = \prod'_{\mathbf{k},\sigma} \frac{1}{\sqrt{2}} (\hat{c}_{\mathbf{k}\sigma}^\dagger + \sigma \hat{c}_{\mathbf{k}+\mathbf{Q},\sigma}^\dagger) |0\rangle. \quad (4.2)$$

Here  $\mathbf{Q} = (\pi, \pi, \dots, \pi)$  is the antiferromagnetic wave vector and the prime indicates that  $\mathbf{k}$  belongs to the magnetic Brillouin zone. The application of the operator  $e^{-\eta\hat{T}}$  to the Néel state yields

$$|\Psi_B\rangle = \prod'_{\mathbf{k},\sigma} \frac{1}{\sqrt{2}} (e^{-\eta\epsilon(\mathbf{k})} \hat{c}_{\mathbf{k}\sigma}^\dagger + \sigma e^{\eta\epsilon(\mathbf{k})} \hat{c}_{\mathbf{k}+\mathbf{Q},\sigma}^\dagger) |0\rangle \quad (4.3)$$

where  $\epsilon(\mathbf{k})$  is the tight-binding spectrum. Eq. (4.3) has the same form as the conventional Hartree-Fock spin density wave state, although with different amplitudes. It is therefore straightforward to calculate the expectation value for the energy. We find

$$\varepsilon_B = \frac{E_B}{L} = \frac{T}{L} + \frac{U}{4} (1 - m^2) \quad (4.4)$$

where

$$T = -L \int_{-\infty}^{\infty} d\epsilon \rho(\epsilon) \epsilon \tanh(2\eta\epsilon) \quad (4.5)$$

is the kinetic energy,

$$m = \int_{-\infty}^{\infty} d\epsilon \rho(\epsilon) \frac{1}{\cosh(2\eta\epsilon)} \quad (4.6)$$

is the sublattice magnetization and  $\rho(\epsilon)$  is the density of states. The variational ground state energy is then obtained by minimizing Eq. (4.4) with respect to  $\eta$ .

We notice that all information about the symmetry and the dimensionality of the lattice is contained in the density of states. For the infinite-dimensional case this quantity has been calculated either by invoking the central-limit theorem [16, 21] or by expanding the Fourier transform of  $\rho(\epsilon)$  in powers of  $1/d$  [22]. In the Appendix the second method is explained and worked out for the two cases of interest. One has to keep in mind that a non-trivial limit is obtained only if the hopping parameter  $t$  is rescaled, as already observed by Metzner and Vollhardt [16]. With the choice  $t = (2d)^{-1/2} t^*$  the density of states for the hypercubic lattice is found to be

$$\rho(\epsilon) = \frac{1}{\sqrt{2\pi} t^*} \exp[-\epsilon^2/2t^{*2}]. \quad (4.7)$$

For the hyperdiamond lattice we choose the scaling  $t = (d/2)^{-1/2}t^*$  and obtain

$$\rho(\epsilon) = \frac{|\epsilon|}{2t^{*2}} \exp[-\epsilon^2/2t^{*2}]. \quad (4.8)$$

For large  $\epsilon$  the two expressions are very similar, however they differ markedly in the limit  $\epsilon \rightarrow 0$ , where the density of states has a maximum for the hypercubic lattice and vanishes for the hyperdiamond lattice.

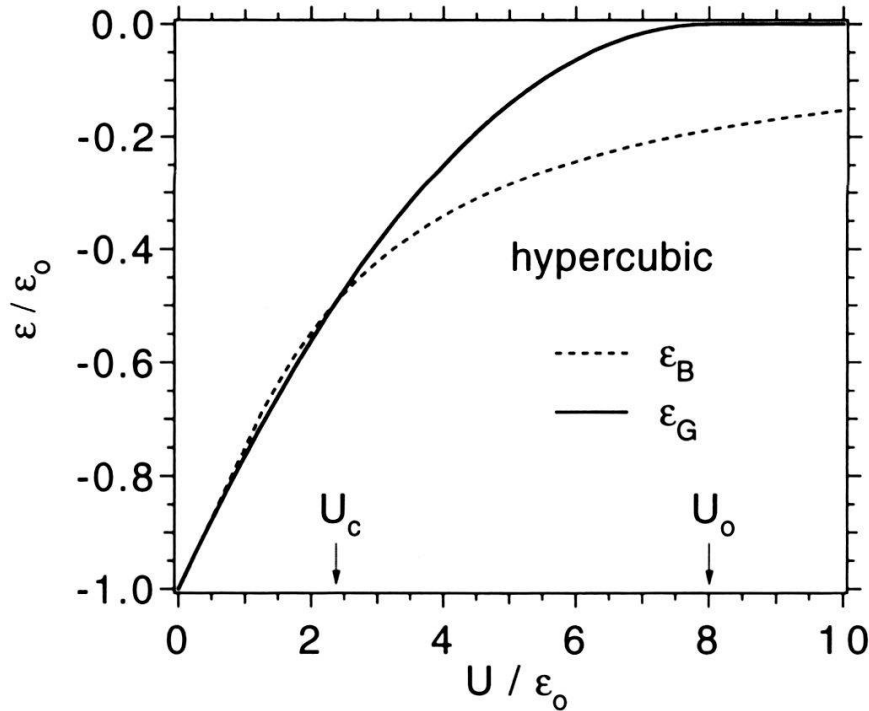


Figure 1: Variational ground state energies for the hypercubic lattice.  $U_c$  indicates the transition from the metallic (full line) to the insulating regime (dashed line).  $U_0$  marks the Brinkman-Rice transition.

We have minimized the variational energy (4.4) with respect to  $\eta$  for these two types of lattices. The results are shown in Figs. 1 and 2 together with the ground state energies of the Gutzwiller approximation (4.1), with  $|\epsilon_0| = (2/\pi)^{1/2}t^*$  for the hypercubic lattice and  $|\epsilon_0| = (\pi/2)^{1/2}t^*$  for the hyperdiamond lattice. The critical value  $U_c$  is seen to be much lower than  $U_0$ , the value of Brinkman and Rice. However it is quite similar in the two cases considered here, namely  $U_c \simeq 2.4|\epsilon_0|$  for the hypercubic lattice and  $U_c \simeq 3.2|\epsilon_0|$  for hyperdiamond. In fact, in both cases it corresponds to an effective bandwidth.

Fig. 3 shows the charge stiffness  $D_c$  and the sublattice magnetization  $m$  for the hyperdiamond lattice. The Gutzwiller ansatz yields a finite Drude weight below the value  $U_0$ , which may be identified with the critical point where the metallic solution is unstable with respect to the Mott phenomenon. With more refined methods this instability point is found to be shifted to slightly lower values [7, 21]. On the other hand the state  $|\Psi_B\rangle$  represents

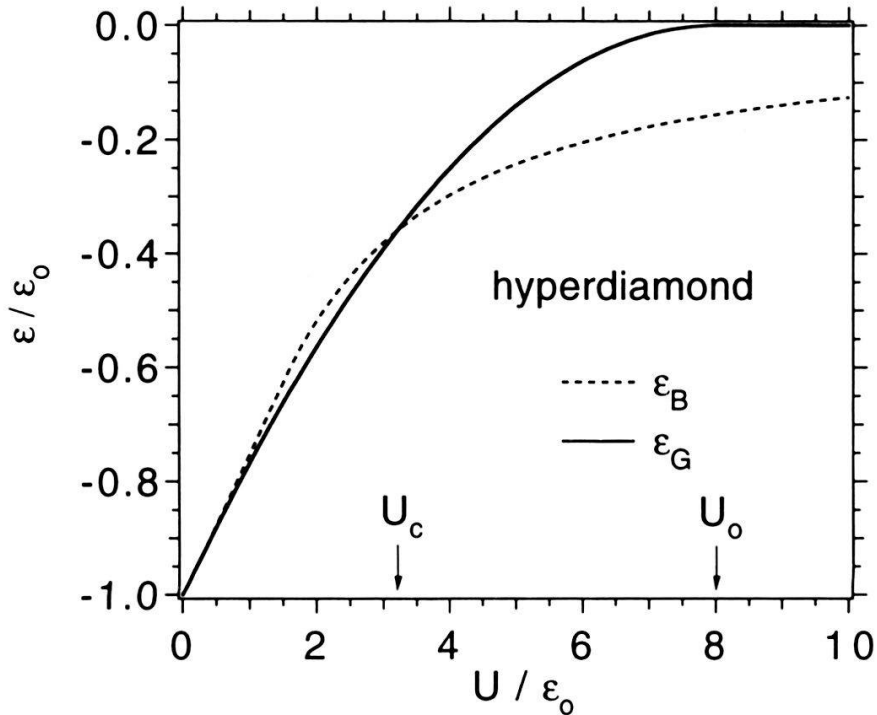


Figure 2: Variational ground state energies for the hyperdiamond lattice.

an antiferromagnetic insulator with a finite sublattice magnetization, which tends to zero as  $U$  approaches  $U_m$  from above. The value  $U_m$  lies below  $U_c$  and corresponds to the magnetic instability of the metal, i.e., the Slater transition. Fluctuations will shift this point to the right, but it is not expected that it will eventually coincide with the (hypothetical) Mott transition.

Within our variational approach there is a single first order transition at  $U_c$  with a jump both in the Drude weight and in the antiferromagnetic order parameter. This behaviour is not expected to survive further refinements of the variational wavefunctions. Indeed, allowing for a spin-density wave in the Gutzwiller ansatz (2.1) would undoubtedly yield a broken symmetry for all  $U > 0$  for the hypercubic lattice and presumably also within some region below  $U_c$  for the hyperdiamond lattice. This will lead to a single Slater-type transition from a paramagnetic metal to an insulating spin-density wave with small moments (at  $U = 0$  in the hypercubic case, at a finite  $U$  in the hyperdiamond case), followed by a continuous crossover to an antiferromagnetic insulator (with nearly saturated moments) around  $U_c$ .

## 5 One dimension

We turn now to the other "solvable" limit, the one-dimensional Hubbard model. In this case strong spin fluctuations preclude antiferromagnetic long-range order, and one can hope to find a Mott-Hubbard transition without further complications. Unfortunately, for the

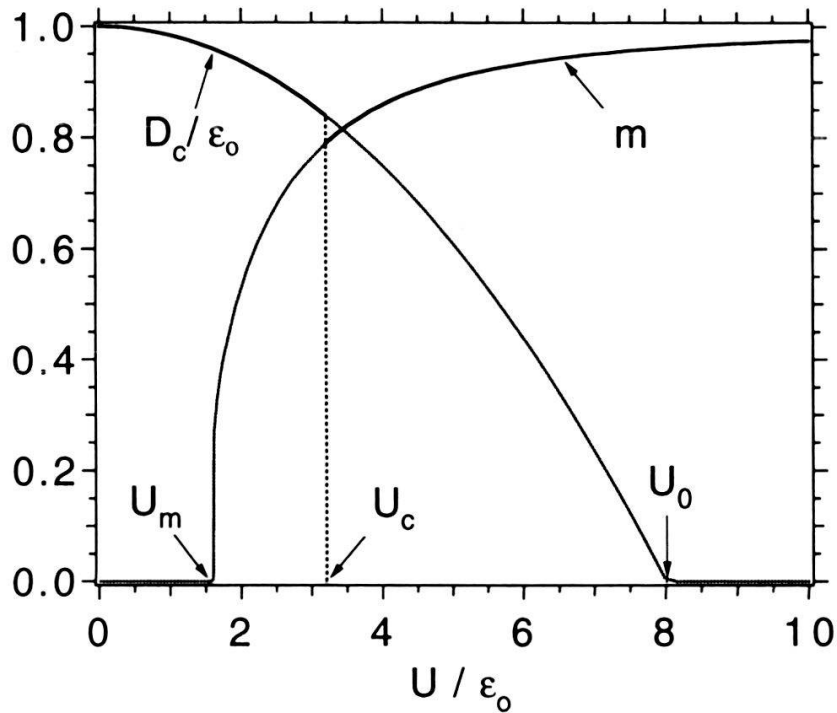


Figure 3: Charge stiffness  $D_c$  and sublattice magnetization  $m$  for the hyperdiamond lattice. The interpretation of the special values  $U_m$ ,  $U_c$ ,  $U_0$  is given in the text.

canonical model with nearest neighbour hopping an infinitesimal positive  $U$  is sufficient for turning the system into an insulator and there is no Mott transition at  $U > 0$  [23].

The addition of hopping between next-nearest neighbour sites (parameter  $t'$ ) is expected to reduce the stability of the insulating phase, but as long as this term does not drastically modify the band structure, the characteristic charge gap of the insulator will remain finite [24]. For large enough values of  $t'$  the Fermi surface (at half filling) consists of four Fermi points and the techniques developed for the normal case of two Fermi points (bosonization and renormalization group [25]) have to be modified. Recent work by Fabrizio indeed shows that for this region of parameters a metallic phase appears below a critical value of  $U$ , above which the system is insulating [26].

A very special model where a Mott-Hubbard transition also occurs at a finite value of  $U$  has been introduced by Gebhard and Ruckenstein [27]. It is defined by a one-dimensional Hubbard Hamiltonian with long-range  $1/r$  hopping

$$t_{j,j+l} = \frac{i\pi t}{L} \frac{(-1)^l}{\sin(\pi l/L)}. \quad (5.1)$$

For antiperiodic boundary conditions and an even number of sites  $L$  the spectrum is linear,  $\epsilon_k = t k$ ,  $-\pi < k < \pi$ , and has a bandwidth  $W = 2\pi t$ . This model is somewhat artificial since the non-interacting ground state has a maximum current. Thus it is not very attractive for studying transport properties. It is convenient to use the symmetrized form of the Hubbard

term,

$$\hat{H}_{int} = U \sum_i (\hat{n}_{i\uparrow} - \frac{1}{2})(\hat{n}_{i\downarrow} - \frac{1}{2}). \quad (5.2)$$

An apparently exact correspondence between the spectra of the  $1/r$  model and the Ashkin-Teller model allows to show that above  $U_c = W$  a charge gap opens (at half-filling), signaling a metal-insulator transition [27]. The ground state energy, given by the simple expression

$$\frac{E_0}{L} = \begin{cases} -\frac{W}{4} - \frac{U^2}{12W} & \text{for } U < W \\ -\frac{U}{4} - \frac{W^2}{12U} & \text{for } U > W \end{cases} \quad (5.3)$$

has a dual form. Given  $E_0$  for  $W = \epsilon_1$ ,  $U = \epsilon_2$  one obtains  $E_0$  for  $W = \epsilon_2$ ,  $U = \epsilon_1$  simply by interchanging  $W$  and  $U$ . It is also possible to calculate explicitly the expectation values for variational wave functions [18]. In our context it is particularly convenient that the state  $|\Psi_\infty\rangle$  is simply obtained as the limit of the Gutzwiller wave function (2.1) for  $\eta \rightarrow \infty$  [28, 29]. Interestingly the two wave functions  $|\Psi_G\rangle$ ,  $|\Psi_B\rangle$  form a dual pair, namely the variational ground state energy  $E_G$  for  $W = \epsilon_1$  and  $U = \epsilon_2$  is the same as the energy  $E_B$  for  $W = \epsilon_2$  and  $U = \epsilon_1$  [30]. Therefore the two energies coincide for  $U = W$ , i.e., at the critical point of the Mott-Hubbard transition. The resulting variational ground state,  $|\Psi_G\rangle$  for  $U < W$ ,  $|\Psi_B\rangle$  for  $U > W$  preserves the duality of the exact solution, thanks to the symmetric roles of the kinetic and the potential energies.

Fig. 4 shows the deviation between the variational results and the exact ground state energy. For  $U < W$  the metallic state  $|\Psi_G\rangle$  is preferred, while for  $U > W$  the insulating state  $|\Psi_B\rangle$  has lower energy. The resulting error is largest at the critical point, which is reminiscent of low- and high-temperature expansions for models of ordinary phase transitions, where the largest uncertainty in the free energy and its derivatives is found at the critical temperature. Fig.4 also illustrates the dual character of the two wave functions. It is worthwhile to add that the variational states  $|\Psi_G\rangle$ ,  $|\Psi_B\rangle$  can be systematically improved by applying in an alternating sequence the two projection operators  $e^{-\eta\hat{D}}$ ,  $e^{-\eta\hat{T}}$ . It turns out that the states involving two projection operators

$$\begin{aligned} |\Psi_{GB}\rangle &= e^{-\eta_2\hat{T}} e^{-\eta_1\hat{D}} |\Psi_0\rangle \\ |\Psi_{BG}\rangle &= e^{-\eta_2\hat{D}} e^{-\eta_1\hat{T}} |\Psi_\infty\rangle \end{aligned} \quad (5.4)$$

form again a dual pair [30]. Therefore the critical point does not move. However the agreement between the variational energy and the exact result is improved by an order of magnitude [30].

The application of an increasing number of these operators amounts to a Trotter decomposition of the operator  $e^{-\beta\hat{H}}$  and is expected to provide wave functions that rapidly converge to the exact ground state (provided that the latter is not orthogonal to the initial trial state).

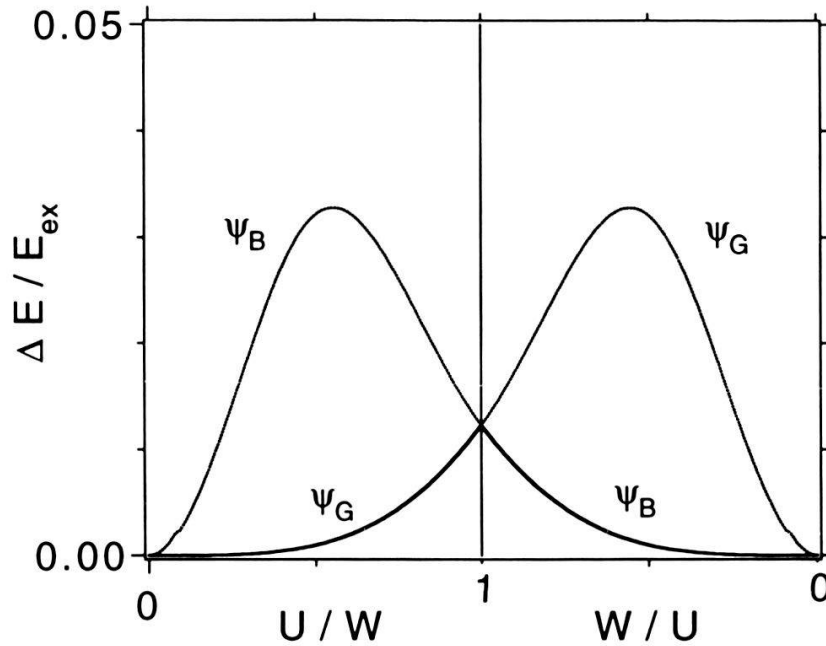


Figure 4: Relative error of the two variational ground state energies for the  $1/r$  model. The full line represents the solution with lower energy, i.e. the metallic state  $|\Psi_G\rangle$  for  $U < W$  and the insulating state  $|\Psi_B\rangle$  for  $U > W$ .

## 6 Conclusions

We have presented a variational study of the Hubbard model at half-filling, using two types of wave functions. The first, introduced many years ago by Gutzwiller, describes a metallic phase, the second, related to the ground state of the Heisenberg model, an antiferromagnetic insulator. We have considered a few special cases in one and infinite dimensions and observed that for small  $U$  the first wave function has lower energy, whereas for large  $U$  the second wave function is preferred. Within this variational scheme a transition between a paramagnetic metal and an antiferromagnetic insulator occurs for  $U \sim W$ . For the  $1/r$  Hubbard chain this value of  $U$  determines also the borderline between the large and small  $U$  regions connected by a duality relation and thus reproduces the exactly known critical point of the Mott-Hubbard transition. On the other hand, in the limit  $d \rightarrow \infty$  the special value of  $U$  found in this way should not be identified with the true metal-insulator transition, because the metallic phase close to this point is expected to be unstable with respect to a spin-density wave. Therefore the true transition will be shifted to lower values of  $U$  and assume the character of a Slater-type magnetic instability, presumably at  $U = 0$  for the hypercubic lattice, but at a finite value for hyperdiamond. This band antiferromagnetism is expected to be stabilized with increasing  $U$ , whereas the antiferromagnetism in the insulating phase will be governed by the energy scale  $t^2/U$ . Therefore we expect that the special value of  $U$  calculated here not only marks the crossover between a spin-density wave and a Heisenberg antiferromagnet, but also corresponds to the point where the critical temperature has a maximum, and where

at still higher temperatures a Mott transition between a paramagnetic metal and a non-magnetic insulator occurs. Further more refined variational calculations will be necessary to substantiate this conclusion. The extension to other dimensions of this approach would also be very interesting, especially to the honeycomb lattice where Monte Carlo simulations indicate that the Mott transition coincides with the Slater instability [31].

## Acknowledgments

This work has been supported by the Swiss National Foundation through the Grant No. 20-40672.94 and by the Junta Nacional de Investigação Científica e Tecnológica (Portugal) through the Grant Praxis XXI/BD/3797/94.

## A Appendix

In this appendix we calculate the density of states for the hypercubic and hyperdiamond lattices in the limit of infinite dimensions, following the method of Müller-Hartmann [22]. The density of states is defined as

$$\begin{aligned}\rho(\epsilon) &= \int_{BZ} \left(\frac{dk}{2\pi}\right)^d \delta(\epsilon - \epsilon_{\mathbf{k}}) \\ &= \int_{BZ} \left(\frac{dk}{2\pi}\right)^d \int_{-\infty}^{\infty} \frac{d\xi}{2\pi} e^{i\xi(\epsilon - \epsilon_{\mathbf{k}})}\end{aligned}\quad (\text{A.1})$$

We first consider the hypercubic lattices, where the tight-binding band structure is additive,

$$\epsilon_{\mathbf{k}} = -2t \sum_{\alpha=1}^d \cos k_{\alpha}.\quad (\text{A.2})$$

Therefore we find

$$\begin{aligned}\rho(\epsilon) &= \int_{-\infty}^{\infty} \frac{d\xi}{2\pi} e^{i\xi\epsilon} \left[ \int_{-\pi}^{\pi} \frac{dk}{2\pi} e^{2i\xi t \cos k} \right]^d \\ &= \int_{-\infty}^{\infty} \frac{d\xi}{2\pi} e^{i\xi\epsilon} [J_0(2\xi t)]^d.\end{aligned}\quad (\text{A.3})$$

For large  $d$  we can expand the Bessel function,  $J_0(x) \simeq 1 - x^2/4 \simeq \exp(-x^2/4)$ , and obtain Eq. (4.7) by using the scaling  $t = (2d)^{-1/2} t^*$ .

The hyperdiamond lattice has a unit cell with two atoms. Therefore the tight-binding spectrum has two branches  $\pm\epsilon_{\mathbf{k}}$ , where

$$\epsilon_{\mathbf{k}} = t \sqrt{\left(1 + \sum_{\alpha=1}^d \cos k_{\alpha}\right)^2 + \left(\sum_{\alpha=1}^d \sin k_{\alpha}\right)^2} \quad (\text{A.4})$$

and  $k_{\alpha}$ ,  $\alpha = 1, \dots, d$ , are the projections of the vector  $\mathbf{k}$  onto the basis vectors of the unit cell. For  $\epsilon > 0$  the density of states per site can be written as

$$\rho(\epsilon) = \frac{1}{2} \int dx \int dy \int \left(\frac{dk}{2\pi}\right)^d \delta\left(x - \sum_{\alpha} \cos k_{\alpha}\right) \delta\left(y - \sum_{\alpha} \sin k_{\alpha}\right) \delta\left(\epsilon - t\sqrt{(1+x)^2 + y^2}\right). \quad (\text{A.5})$$

Introducing the representation

$$\delta(x - x_0) = \int \frac{d\xi}{2\pi} e^{i\xi(x-x_0)} \quad (\text{A.6})$$

we again obtain an expression where the  $k$ -integration can be factorized

$$\rho(\epsilon) = \frac{1}{2} \int dx \int dy \delta\left(\epsilon - t\sqrt{(1+x)^2 + y^2}\right) \int \frac{d\xi}{2\pi} \int \frac{d\eta}{2\pi} e^{i\xi x} e^{i\eta y} I^d \quad (\text{A.7})$$

where

$$I = \int_{-\pi}^{\pi} \frac{dk}{2\pi} e^{-i(\xi \cos k + \eta \sin k)} = J_0(\sqrt{\xi^2 + \eta^2}). \quad (\text{A.8})$$

For large  $d$  the leading contribution again comes from small arguments of the Bessel function

$$J_0(\sqrt{\xi^2 + \eta^2}) \simeq 1 - \frac{1}{4}(\xi^2 + \eta^2) \simeq e^{-\frac{1}{4}(\xi^2 + \eta^2)}. \quad (\text{A.9})$$

It is then straightforward to perform the remaining integrals, giving

$$\rho(\epsilon) = \frac{1}{2} \int dx \int dy \delta\left(\epsilon - t\sqrt{(1+x)^2 + y^2}\right) \frac{1}{\pi d} e^{-(x^2+y^2)/d}. \quad (\text{A.10})$$

In the limit  $d \rightarrow \infty$  we obtain

$$\rho(\epsilon) = \frac{1}{d t^2} \epsilon e^{-\frac{\epsilon^2}{4t^2}}. \quad (\text{A.11})$$

The scaling  $t = (d/2)^{-1/2} t^*$  then immediately leads to Eq. (4.8). For  $\epsilon < 0$  one simply uses the electron-hole symmetry,  $\rho(\epsilon) = \rho(-\epsilon)$ .



## References

- [1] N. F. Mott, *Metal-Insulator Transitions*, Taylor and Francis (London 1990).
- [2] N. F. Mott, Proc. Phys. Soc. **A62**, 416 (1949).
- [3] J. Hubbard, Proc. Roy. Soc. **A276**, 238 (1963).
- [4] W. F. Brinkman and T. M. Rice, Phys. Rev. B **2**, 4302 (1970).
- [5] P. W. Anderson, in *Frontiers and Borderlines in Many-Particle Physics*, edited by R. A. Broglia and J. R. Schrieffer, North-Holland (Amsterdam 1988), p. 1.
- [6] J. C. Slater, Phys. Rev. **82**, 538 (1951).
- [7] A. Georges, G. Kotliar, W. Krauth and M. J. Rozenberg, Rev. Mod. Phys. **68**, 13 (1996).
- [8] M. C. Gutzwiller, Phys. Rev. Lett. **10**, 159 (1963).
- [9] M. C. Gutzwiller, Phys. Rev. **134**, A923 (1964), *ibid.* **137**, A1726 (1965).
- [10] T. Kaplan, P. Horsch, and P. Fulde, Phys. Rev. Lett. **49**, 889 (1982).
- [11] H. Yokoyama and H. Shiba, J. Phys. Soc. Japan **59**, 3669 (1990).
- [12] P. Fazekas and K. Penc, Int. J. Mod. Phys. B **2**, 1021 (1988).
- [13] D. Baeriswyl, in: *Nonlinearity in Condensed Matter*, eds. A. R. Bishop *et al.*, Springer Series in Solid State Sciences **69**, p. 183 (1987).
- [14] W. Kohn, Phys. Rev. **133**, A171 (1964).
- [15] A. J. Millis and S. N. Coppersmith, Phys. Rev. B **43**, 13770 (1991).
- [16] W. Metzner and D. Vollhardt, Phys. Rev. Lett. **62**, 324 (1989).
- [17] W. Metzner and D. Vollhardt, Phys. Rev. Lett. **59**, 121 (1987); Phys. Rev. B **37**, 7382 (1988); Erratum Phys. Rev. B **39**, 12339 (1989).
- [18] F. Gebhardt and A. Girndt, Z. Phys. B **93**, 455 (1994).
- [19] H. Yokoyama and H. Shiba, J. Phys. Soc. Japan. **56**, 1490 (1987).
- [20] T. Kennedy, E. H. Lieb and B. S. Shastry, Phys. Rev. Lett. **61**, 2582 (1988).
- [21] G. Santoro, M. Airoldi, S. Sorella and E. Tosatti, Phys. Rev. B **47**, 16 216 (1993).
- [22] E. Müller-Hartmann, Z. Phys. B, **74**, 507 (1989).
- [23] E. H. Lieb and F. Y. Wu, Phys. Rev. Lett. **20**, 1445 (1968).

- [24] V. J. Emery, A. Luther and I. Peschel, *Phys. Rev. B* **13**, 1272 (1976).
- [25] J. Solyom, *Adv. Phys.* **28**, 201 (1979).
- [26] M. Fabrizio, SISSA Preprint no. 30/96/CM/MB.
- [27] F. Gebhardt and A. Ruckenstein, *Phys. Rev. Lett.* **68**, 244 (1992).
- [28] F. D. M. Haldane, *Phys. Rev. Lett.* **60**, 635 (1988).
- [29] B. S. Shastry, *Phys. Rev. Lett.* **60**, 638 (1988).
- [30] M. Dzierzawa, D. Baeriswyl and M. Di Stasio, *Phys. Rev. B* **51**, 1993 (1995).
- [31] S. Sorella and E. Tosatti, *Europhys. Lett.* **19**, 699 (1992).